

Molecular conduction: Do time-dependent simulations tell you more than the Landauer approach?

Cristián G. Sánchez^{a)}

Unidad de Matemática y Física, Facultad de Ciencias Químicas, INFIQC, Universidad Nacional de Córdoba, Ciudad Universitaria, 5000 Córdoba, Argentina

Maria Stamenova and Stefano Sanvito

School of Physics, Trinity College, Dublin 2, Ireland

D. R. Bowler and Andrew P. Horsfield

Department of Physics and Astronomy, University College London, Gower Street, London WC1E 6BT, United Kingdom

Tchavdar N. Todorov

Atomistic Simulation Centre, Queen's University Belfast, Belfast BT7 1NN, United Kingdom

(Received 10 March 2006; accepted 11 April 2006; published online 7 June 2006)

A dynamical method for simulating steady-state conduction in atomic and molecular wires is presented which is both computationally and conceptually simple. The method is tested by calculating the current-voltage spectrum of a simple diatomic molecular junction, for which the static Landauer approach produces multiple steady-state solutions. The dynamical method quantitatively reproduces the static results and provides information on the stability of the different solutions. © 2006 American Institute of Physics. [DOI: 10.1063/1.2202329]

I. INTRODUCTION

Recently, there has been a surge of interest in time-dependent (TD) simulations of current-carrying molecular devices, from a variety of points of view.^{1–11} The well-known static Landauer-Büttiker picture is an invaluable tool for the description of steady-state conduction. What can dynamical transport simulations add? They are required to describe the transient response to an external perturbation. A practical nanodevice of necessity relies for its operation on the implementation and function of a switch (a short-lived external signal that can change the state and mode of operation of the device).¹² Transport in systems at this size scale is not necessarily always a steady-state process, with the possibility of intrinsic dynamical fluctuations and instabilities in the flow pattern and in the underlying transport mechanism.

A further motivation behind the TD approach to transport is the problem of current-driven mechanical effects. Recently, we have proposed a method for quantum correlated electron-ion molecular dynamics.¹³ Among other effects, this method enables the simulation of inelastic electron-phonon interactions, dissipation, local heating, and inelastic I - V spectroscopy within the framework of molecular dynamics. A key step on the way is to combine tractable dynamics with steady-state conditions. We have developed an open-boundary scheme that achieves this by opening the system to a voltage source.^{3,14} Here, we report an open-boundary dynamical scheme that relies on opening the system to a charge source. The advantage of the present method is its great conceptual and computational simplicity.

The method is tested on a simple molecular junction, for

which the static Landauer approach produces multiple steady-state solutions, corresponding to different transport mechanisms. The dynamical method quantitatively reproduces these results. It furthermore shows which the preferred, or more stable, steady-state solutions are, as a function of bias.

II. DYNAMICAL METHOD

We consider the *finite* system shown in Fig. 1. It consists of a capacitor C , connected by a pair of leads to a device D .^{1,5} Initially (at $t=t_0$) the system is statically polarized to produce a charge imbalance between the plates of the capacitor. This can be achieved by exposing the system to a static external field, such as would be produced by a thin dipolar layer placed between the plates.

At $t > t_0$ the external field is removed over a short time and the system, which is no longer in a stationary state, is allowed to evolve according to the following equation of motion:

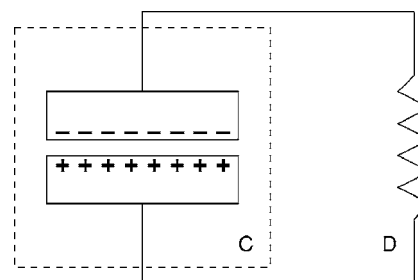


FIG. 1. Division of the system into capacitor and device

^{a)}Electronic mail: cgsanchez@fcq.unc.edu.ar

$$\frac{\partial \hat{\rho}}{\partial t} = \frac{1}{i\hbar} [\hat{H}[\hat{\rho}], \hat{\rho}]. \quad (1)$$

Here, $\hat{\rho} = \hat{\rho}(t)$ is the reduced spinless one-particle electronic density matrix (DM) and $\hat{H}[\hat{\rho}]$ is a generic effective one-electron Hamiltonian, such as that produced by time-dependent density-functional theory¹⁵ (TDDFT) or, in a many-body framework, by the Hartree-Fock approximation for the two-electron DM. In a TDDFT framework we have the assurance that if we partition the system into two subregions (such as one plate plus some of the adjoining lead, and the rest), then the *total* particle current between them, computed from the one-electron DM, is formally exact.^{4,5}

Although the above scheme is conceptually feasible, the capacitor sizes needed to provide discharge times significantly exceeding the femtosecond range, limit its practical use. A solution is to continually feed electrons that have flown across back into the starting electrode. Classically, this is easy. Quantum mechanically, it is easier said than done. The reason is not *necessarily* that electrons are not sufficiently particlelike to enable such an action, but that the quantum *description* of electrons prohibits moving them about one by one, in a literal sense, in a calculation. Therefore, we maintain the charge imbalance, and hence the current, in the system by a driving term that achieves what we require at the level of the DM,

$$\frac{\partial \hat{\rho}}{\partial t} = \frac{1}{i\hbar} [\hat{H}[\hat{\rho}], \hat{\rho}] - \Gamma(\hat{\rho} - \hat{\rho}^0), \quad (2)$$

where Γ is a real parameter, and the operator $\hat{\rho}^0$ is defined in terms of its matrix elements in some real-space basis as

$$\rho_{ij}^0 = \begin{cases} \rho_{ij}(t_0) & \text{for } i, j \in C \\ \rho_{ij}(t) & \text{otherwise.} \end{cases} \quad (3)$$

The new term in the equation of motion continually drives the DM in the capacitor region back toward the initial polarized density matrix. Physically, this achieves two things. First, it describes the effect of connecting the capacitor to an external charge source that maintains the charge imbalance in the system. Second, since $\hat{\rho}(t_0)$ is purely real, it damps the imaginary parts of $\hat{\rho}$ in the capacitor region and thus incorporates into the description of the electrons a generic phase-breaking scattering mechanism in the electrodes. If Γ is too small, this suppresses the current, due to a suppression of the first effect. If Γ is too large, that suppresses the current, due to an enhancement of the second effect. For the simulations below, we have used the compromise value of Γ ($\Gamma = 4 \text{ fs}^{-1}$ for the specific system considered later). The appendixes show that the time-dependent equation has a simple heuristic interpretation and that the steady-state solutions to Eq. (2) correspond to the static Landauer picture under specific approximations. Further, a derivation of the microscopic origin and value of the parameter Γ is given.

As a test we have implemented the scheme above in an orthogonal tight-binding model with mean-field interactions, with

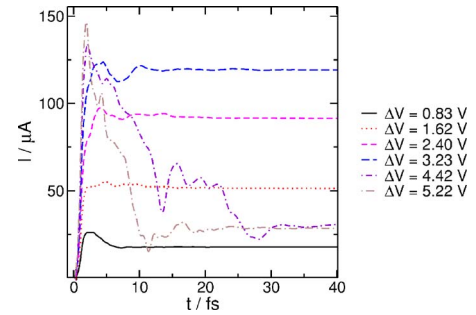


FIG. 2. Current as a function of time from the integration of Eq. (2). The bias shown corresponds to the final steady state.

$$\hat{H} = \sum_{i \neq j} |i\rangle H_{ij} \langle j| + \sum_i |i\rangle \left(U \Delta q_i + \sum_{j \neq i} f_{ij} \Delta q_j \right) \langle i|, \quad (4)$$

where $\Delta q_i = 2(\rho_{ii} - 1/2)$. The function of interatomic separation $f_{ij} = K / \sqrt{R_{ij}^2 + K^2/U^2}$, with $K = e^2/4\pi\epsilon_0$, interpolates smoothly between onsite interactions with a strength U and the bare Coulomb interaction at large separation. This model may be viewed as the simplest form of TDDFT in the adiabatic local-density approximation (ALDA).¹⁶ In the simulations below, $U = 7 \text{ eV}$.¹⁷

We consider the following model system. The capacitor plates are two-dimensional (2D) (one-atom thick) 15×20 -atom simple-cubic slabs, in the plane of the page, the leads are 15-atom long one-dimensional (1D) atomic chains, and the device is a dimer. The only nonzero hopping integrals are those between nearest neighbors. The latter are everywhere equal to -3.88 eV , except each dimer-lead hopping integral (-1 eV), and the intradimer hopping integral (also -1 eV).

The external field at t_0 is imposed as a rigid relative shift of the onsite energies in the capacitor plates, as described in Ref. 13. After removing the external bias, Eq. (2) is integrated using the method described in Ref. 14. The current flowing through the dimer as a function of time is shown in Fig. 2 for different applied biases. After an initial transient, the current settles at a steady state. The bias is calculated from the average onsite energy in each plate at the end of the simulation and is smaller than the applied bias, mainly due to the finite size of the capacitor. For small bias, the steady state is reached after a short rising transient of about 10 fs. For biases larger than about 4 V, the current first rises up to about $120 \mu\text{A}$ and then gradually decreases to reach a much lower value of about $25 \mu\text{A}$ in the steady state. The I - V spectrum obtained from the steady-state current and potential difference is shown in Fig. 3. Up to $V \sim 4 \text{ V}$ the spectrum has the structure expected for resonant transmission (see discussion below). However, we then see a sudden drop in current, with heavily suppressed conduction at higher bias. With the present parameters, the bandwidth in the 2D plates is $\sim 31 \text{ eV}$ and in the 1D leads it is $\sim 16 \text{ eV}$. Therefore, the reason for the I - V spectrum above cannot be that device states float out of the conduction bands of the electrodes. Changing the value of Γ from 4 to 3 fs^{-1} has no significant effect, as can be seen from the plot.

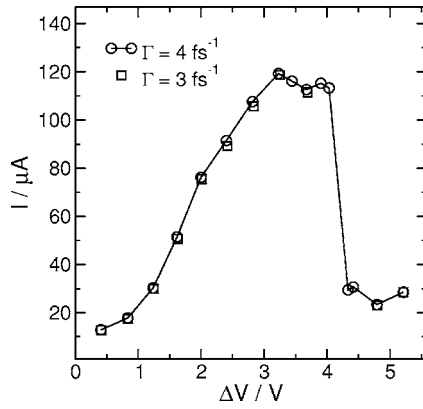


FIG. 3. Current-voltage curve obtained from the final values of the current and potential difference after a steady state has been reached, for two different values of the parameter Γ .

III. DISCUSSION

To understand these results, we now put our system through the machinery of the Landauer formalism. First, we consider an approximate semianalytical solution. Later, we confirm it by a fully self-consistent Landauer calculation. We consider a dimer between two semi-infinite linear atomic chains. The dimer hopping integral is δ , the dimer-lead hopping integrals are γ , and the hopping integral in each lead is β . The Fermi level in the absence of current is chosen as zero. The left lead is open to a reservoir with electrochemical potential $eV/2$ and the right lead is open to a reservoir with electrochemical potential $-eV/2$. $V > 0$ corresponds to electron flow from left to right. We neglect Friedel oscillations in the leads and assign a uniform onsite energy E_L to the left lead and E_R to the right lead. The onsite energies of the dimer atoms are E_1 and E_2 . The steady-state electronic structure requires only the self-consistent Hamiltonian and Green's function for the current-carrying system. To generate the latter, we use a familiar construct: A fictitious system with all hopping integrals and onsite energies as above but with the hopping integral between the two dimer atoms removed. Let $\hat{G}_L^{0+}(E)$ and $\hat{G}_R^{0+}(E)$ be the retarded Green's functions for the two decoupled semi-infinite systems thus obtained. We will, in fact, only ever need the matrix elements $(G_L^{0+})_{11} = 1/[E - E_1 - \gamma^2 g_L^+(E)]$, $(G_R^{0+})_{22} = 1/[E - E_2 - \gamma^2 g_R^+(E)]$, on the respective dimer sites. Here, g_L^+ and g_R^+ are the onsite matrix elements of the retarded Green's functions on the end site of each bare lead, given by $g_{L(R)}^+ = [E - E_{L(R)} \pm \sqrt{(E - E_{L(R)})^2 - 4\beta^2}]/2\beta^2$, where we choose the minus sign if the expression under the square root is negative, while if this expression is positive, we choose the minus sign if $(E - E_{L(R)}) > 0$ and the plus sign if $(E - E_{L(R)}) < 0$.^{18,19} The DM for the current-carrying system in the steady state is given by²⁰

$$\hat{\rho} = \int_{-\infty}^0 \hat{D}(E) dE - \int_{-eV/2}^0 \hat{D}_R(E) dE + \int_0^{eV/2} \hat{D}_L(E) dE. \quad (5)$$

Here, $2\pi i \hat{D}(E) = \hat{G}^-(E) - \hat{G}^+(E)$, $\hat{D}_{L(R)}(E) = \hat{\Omega}(E) \hat{D}_{L(R)}^0(E) \hat{\Omega}(E)^\dagger$, $2\pi i \hat{D}_{L(R)}^0(E) = \hat{G}_{L(R)}^{0-}(E) - \hat{G}_{L(R)}^{0+}(E)$, and $\hat{\Omega}(E) = \hat{1} + \hat{G}^+(E) \hat{V}$, where $\hat{G}^\pm(E)$ are the retarded and ad-

vanced Green's functions for the fully coupled current-carrying system, and \hat{V} is an operator whose only nonzero matrix elements are $V_{12} = V_{21} = \delta$. $\hat{G}^\pm(E)$ solves $\hat{G}^\pm(E) = \hat{G}^{0\pm}(E) + \hat{G}^{0\pm}(E) \hat{V} \hat{G}^\pm(E)$, where $\hat{G}^{0\pm}(E) = \hat{G}_L^{0\pm}(E) + \hat{G}_R^{0\pm}(E)$. The current $I = \text{Tr}[\hat{I} \hat{\rho}]$, where \hat{I} is the tight-binding current operator, is given by¹⁹

$$I = \frac{2e}{h} 4\pi^2 \int_{-eV/2}^{eV/2} (D_L^0)_{11} (D_R^0)_{22} |t_{12}(E)|^2 dE, \quad (6)$$

where $\hat{t}(E) = \hat{V} + \hat{V} \hat{G}^+(E) \hat{V}$. This procedure may be expressed in several algebraically equivalent alternative forms,²¹ equivalent also²² to the non-equilibrium Green's functions (NEGF) (Keldysh) formalism.

Electron-electron interactions in the dimer take the mean-field form $E_{1(2)} = 2U(n_{1(2)} - 1/2)$ where $n_1 = \rho_{11}$ and $n_2 = \rho_{22}$ are the (spinless) electron occupancies of the two dimer sites. The present system has perfect electron-hole symmetry and so we write $n_1 = 1 - n_2 = n$, $E_1 = -E_2 = \epsilon$. In principle, the onsite energies in the 1D leads, $E_L = E_L(V)$ and $E_R = E_R(V)$, must be determined self-consistently.²³ However, we have checked that, for the present model system, the extreme cases $E_L = E_R = 0$ (strictly valid in the limit of perfect transmission) and $E_L = -E_R = eV/2$ (strictly valid in the limit of zero transmission) produce similar I - V characteristics. The results from the semianalytical model below are for $E_L = -E_R = eV/2$. Finally, self-consistency takes the form $n = \rho_{11}(\epsilon) = \epsilon/2U + 1/2$ which is an equation for ϵ , for every bias.²⁴

Let us try to anticipate the behavior of this system. There are two extremes. If the coupling between the two dimer atoms is much weaker than the dimer-lead coupling ($|\delta| \ll |\gamma|$), then the dimer atoms would view themselves as two adsorbates, one on each lead. As the bias increases, each adsorbate tends to remain pinned against the quasi-Fermi level in its lead, with $E_1 \sim eV/2 \sim -E_2$ and with the formation of a corresponding charge dipole in the dimer with an electron excess on the atom facing the incoming electron current. The assembly then conducts by a mechanism akin to the scanning tunneling microscope (STM): adsorbate-adsorbate tunneling, modulated by the convolution of the two adsorbate local densities of states (LDOSs). In particular, once eV exceeds the width of the two LDOSs, and the two adsorbates become mismatched in energy, the current drops and decreases further with increasing V . In the other extreme ($|\delta| \gg |\gamma|$), the dimer behaves as a molecule weakly interacting with two banks. The transport mechanism now is resonant transmission through the bonding and antibonding molecular orbitals. The dimer atoms remain largely neutral and the dimer onsite energies remain largely level. The current increases sharply when V matches the gap between the two molecular orbitals, and saturates for larger V , once both resonances are fully conducting.

In the intermediate case ($|\delta| \sim |\gamma|$), the system suffers an "identity crisis," with the possibility that different transport mechanisms may become operative at different voltages, and that there may be more than one steady-state solution at certain voltages. This is precisely what happens. Figure 4(a)

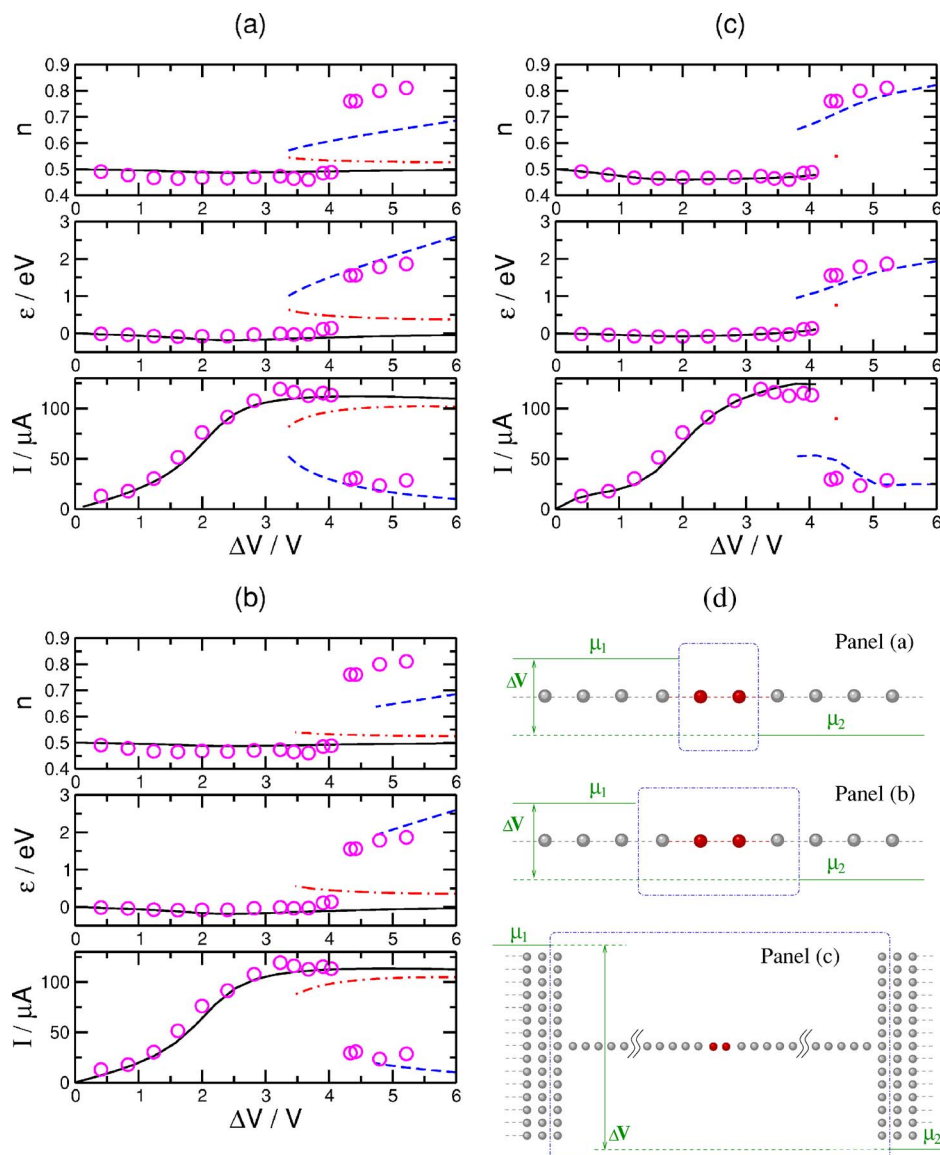


FIG. 4. Spinless onsite occupancy (top panel) and onsite energy (middle panel) on dimer atom 1 (facing the electron current), together with the total current (bottom panel), as a function of bias. Lines are the different Landauer steady state solutions: (a) semianalytical solution, (b) full self-consistent solution with the parameters of the semianalytical model, and (c) full self-consistent solution with 2D electrodes and with the parameters of the time-dependent simulation. Circles are solutions of the time-dependent calculation. (d) Scheme of the systems considered in the other panels. Self-consistent region framed.

shows n , ϵ , and I as a function of V for $\beta = -3.88$ eV, $\gamma = \delta = -1$ eV, and $U = 7$ eV. The solution with high current and low n is the resonant-transmission solution (continuous line). The solution (which appears above $V \sim 3.3$ V) with low current, a dipole (with electron excess on the dimer atom facing the electron current), and ϵ more or less pinned against $eV/2$ is the STM-like solution (dashed line). We will not focus on the intermediate third solution (dot-dashed line).

We see that the dynamical method reproduces parts of each static solution with quantitative accuracy. The difference in n between the TD calculation and the semianalytical model for the blocked solution is due to the screening provided by the intersite Coulomb terms in the TD calculation. The TD calculation naturally selects the low-current solution, above a certain bias. The reason for this preference is the increasing instability, with increasing bias, of the high-current solution against spontaneous charge fluctuations in the dimer: If a small fluctuation in n pushes ϵ away from the special value needed for resonant transmission, this kills the resonance, the current drops, and the system floats to the insulating, STM-like mode, with no recovery mechanism.

To check the above semianalytical model, we have also carried out a fully self-consistent NEGF calculation²⁵ [Figs. 4(b) and 4(c)]. Panel 4(b) pictures the I - V curves for the one-dimensional model system described above. While in the semianalytical approach the region where the density is determined self-consistently consists only of the dimer [see Fig. 4(d)], here the two outmost atoms from the leads are also included in the self-consistency. The three branches from panel (a) are almost fully and exactly reproduced in a series of calculations with randomized initial density matrices for each voltage point. In panel 4(c) the self-consistent region is further extended to resemble as much as possible the system treated with the time-dependent approach [see Figs. 4(c) and 4(d)] and the Hamiltonian from the semianalytical model is augmented with the intersite mean-field interactions [see Eq. (4)]. The onsite occupancy on the dimer n in this case agrees better with the TD simulation and the I - V branches fit better to the TD ones at low bias. Parts of all anticipated branches are recovered and regions of multiple solutions are observed.

Finally, we observe that the agreement between the dy-

namical ALDA calculation and the static Landauer calculation above corroborates the conjecture that the equivalence between TDDFT in ALDA and the Landauer formalism that has recently been demonstrated in the linear-response regime^{26,27} carries over to higher orders in the bias. In addition, the time-dependent approach is able to self-select the most stable solution, when there are multiple values of the current for the same applied bias. This goes beyond the capabilities of static methods, which, in the absence of a total energy criterion, say little about the relative stability of multiple solutions.

ACKNOWLEDGMENTS

One of the authors (C.G.S.) is grateful to CONICET for support. Two of the authors (M.S. and S.S.) thank the Irish Higher Educational Authority (North South Programme for Collaborative Research) for financial support. Another author (D.R.B.) was supported by the Royal Society. Parts of this work were supported by EPSRC under Grant No. GR/R36077. We thank P. Delaney, K. Burke, and M. Di Ventra for helpful discussions.

APPENDIX A: HEURISTIC DERIVATION OF THE DAMPED EQUATION OF MOTION

The use of a damping term in the equation of motion (2) for the one-particle density matrix provides an approximate description of the influence of the environment on the piece of the system that we are interested in (the device). This approximation has a clear physical interpretation which allows us to understand under what conditions the approximation should apply, and assign an order of magnitude to the central parameter Γ .

The starting equation is the Liouville equation for the propagation of the one-particle density matrix by a one-particle Hamiltonian,

$$\frac{\partial \hat{\rho}}{\partial t} - \frac{1}{i\hbar} [\hat{H}, \hat{\rho}] = 0.$$

By separating our system into device and environment we can partition our density matrix accordingly, and obtain an equation of motion for the density matrix within the device region,

$$\frac{\partial \hat{\rho}_{DD}}{\partial t} - \frac{1}{i\hbar} [\hat{H}_{DD}, \hat{\rho}_{DD}] = \frac{1}{i\hbar} (\hat{H}_{DE} \hat{\rho}_{ED} - \hat{\rho}_{DE} \hat{H}_{ED}), \quad (\text{A1})$$

where $\hat{\rho}_{DD}$ (\hat{H}_{DD}) corresponds to the section of the density matrix (the Hamiltonian) solely in the device region, and $\hat{\rho}_{DE} = \hat{\rho}_{ED}^\dagger$ ($\hat{H}_{DE} = \hat{H}_{ED}^\dagger$) is the part of the density matrix (the Hamiltonian) which links the device to the environment. We see that the environment operates as a driving term on the device. To proceed further, it is easiest to represent the Hamiltonian and the density matrix by matrices in which indices α correspond to the device region and indices β correspond to the environment. Thus we obtain for the $\alpha\alpha'$ component of the right-hand side of Eq. (A1),

$$(\text{RHS})_{\alpha\alpha'} = \frac{1}{i\hbar} \sum_{\beta} (H_{\alpha\beta} \rho_{\beta\alpha'} - \rho_{\alpha\beta} H_{\beta\alpha'}). \quad (\text{A2})$$

The easiest terms to interpret are the diagonal ones,

$$\begin{aligned} (\text{RHS})_{\alpha\alpha} &= \frac{1}{i\hbar} \sum_{\beta} (H_{\alpha\beta} \rho_{\beta\alpha} - \rho_{\alpha\beta} H_{\beta\alpha}) \\ &= \frac{2}{\hbar} \sum_{\beta} H_{\alpha\beta} \text{Im}\{\rho_{\beta\alpha}\}, \end{aligned} \quad (\text{A3})$$

where we have assumed that the Hamiltonian is real. This expression gives the rate of charge injection into orbital α (on the device) by the environment. The Hamiltonian is short ranged and we assign an order of magnitude to it by writing $\hbar\Gamma V_{\alpha\beta} = H_{\alpha\beta}$. Here, $V_{\alpha\beta}$ is dimensionless, and takes care of all the angular dependence of the hopping integrals. Then Eq. (A3) becomes

$$(\text{RHS})_{\alpha\alpha} = 2\Gamma \sum_{\beta} V_{\alpha\beta} \text{Im}\{\rho_{\beta\alpha}\}. \quad (\text{A4})$$

When the system is in its initial state (represented by $\hat{\rho}_{DD}^0$) the left-hand side is zero by construction (at least close to the interface with the environment: away from the interface the removal of the charge-separation potential could lead to currents). Since in this initial state there is no net current from the environment into the device (any such current needs time to develop), the right-hand side must also be zero. Therefore, any net flow of charge from the environment into the device must be as a consequence of deviations of the device density matrix away from its initial value. We can combine these observations into a single ansatz, namely,

$$\text{RHS} = \begin{cases} -\Gamma(\hat{\rho}_{DD} - \hat{\rho}_{DD}^0) & \text{near the interface} \\ 0 & \text{away from the interface.} \end{cases} \quad (\text{A5})$$

APPENDIX B: CONSISTENCY WITH THE LANDAUER FORMALISM

Next, we wish to relate Eq. (2) to the static Landauer picture. We will do that by showing—subject to approximations to be determined—that the Landauer steady state is a steady-state solution to Eq. (2).

Consider an electrode-device-electrode system carrying a steady-state current, in the Landauer picture. Select a region S , composed of the device and some extended but finite section of each adjoining electrode. Let \hat{H}_S be the subblock of the self-consistent Hamiltonian for the current-carrying system, within S . Let $\hat{G}_S(z)$ be the Green's function for the current-carrying system, within S . It solves

$$\hat{G}_S(z)[z - \hat{H}_S - \hat{\Sigma}(z)] = \hat{1},$$

where

$$\hat{\Sigma}(z) = \hat{V} \hat{g}_1(z) \hat{V} + \hat{V} \hat{g}_2(z) \hat{V} = \hat{\Sigma}_1(z) + \hat{\Sigma}_2(z).$$

Here, \hat{V} is the Hamiltonian that couples S to the rest, and $\hat{g}_1(z)$ and $\hat{g}_2(z)$ are the Green's functions for the bare left and right semi-infinite pieces that would be left behind if we dug out region S .

The density matrix for the current-carrying system in region S is given by

$$\hat{\rho}_S = \bar{\rho}_S + \Delta\hat{\rho}_S,$$

where

$$\bar{\rho}_S = \frac{1}{2\pi i} \oint \hat{G}_S(z) dz = \int_{-\infty}^{\mu} \hat{D}_S(E) dE, \quad (\text{B1})$$

and

$$\begin{aligned} \Delta\hat{\rho}_S = & \int_{\mu}^{\mu+eV/2} \frac{1}{\pi} \hat{G}_S^+(E) \hat{\sigma}_1(E) \hat{G}_S^-(E) dE \\ & - \int_{\mu-eV/2}^{\mu} \frac{1}{\pi} \hat{G}_S^+(E) \hat{\sigma}_2(E) \hat{G}_S^-(E) dE. \end{aligned} \quad (\text{B2})$$

Here, $\hat{G}_S^{\pm}(E) = \lim_{\epsilon \rightarrow 0^+} \hat{G}_S(E \pm i\epsilon)$, $\hat{D}_S(E) = [\hat{G}_S^-(E) - \hat{G}_S^+(E)] / 2\pi i$, the contour cuts the real axis at the Fermi level μ , for the unbiased system, V is the bias, and

$$\hat{\sigma}_j(E) = \frac{\hat{\Sigma}_j^-(E) - \hat{\Sigma}_j^+(E)}{2i}, \quad j = 1, 2,$$

where $\hat{\Sigma}_j^{\pm}(E) = \lim_{\epsilon \rightarrow 0^+} \hat{\Sigma}_j(E \pm i\epsilon)$.

Consider $[\hat{H}_S, \hat{\rho}_S]$. First consider

$$\begin{aligned} & \frac{1}{i\hbar} [\hat{H}_S, \Delta\hat{\rho}_S] \\ &= -\frac{1}{i\hbar} \left(\int_{\mu}^{\mu+eV/2} \frac{1}{\pi} \hat{\sigma}_1(E) \hat{G}_S^-(E) dE - \text{H.c.} \right) \\ &+ \frac{1}{i\hbar} \left(\int_{\mu-eV/2}^{\mu} \frac{1}{\pi} \hat{\sigma}_2(E) \hat{G}_S^-(E) dE - \text{H.c.} \right) \\ &- \frac{1}{i\hbar} \left(\int_{\mu}^{\mu+eV/2} \frac{1}{\pi} \hat{\Sigma}^+(E) \hat{G}_S^+(E) \hat{\sigma}_1(E) \hat{G}_S^-(E) dE - \text{H.c.} \right) \\ &+ \frac{1}{i\hbar} \left(\int_{\mu-eV/2}^{\mu} \frac{1}{\pi} \hat{\Sigma}^+(E) \hat{G}_S^+(E) \hat{\sigma}_2(E) \hat{G}_S^-(E) dE - \text{H.c.} \right). \end{aligned}$$

We now make our principal approximation. Let \hat{q} be a Green's function or a density matrix. Then, at least locally,

$$\hat{\Sigma}_j^- \hat{q} \approx \gamma_j \hat{q}^{(j)}, \quad \hat{\Sigma}_j^+ \hat{q} \approx \gamma_j^* \hat{q}^{(j)}, \quad j = 1, 2, \quad (\text{B3})$$

where γ_j is an energy-independent scalar and $\hat{q}^{(j)}$ is the projection of \hat{q} in some extended but finite region in the vicinity of the points to which $\hat{\Sigma}_j$ couples. Physically, in this approximation we ignore the atomistic detail of the coupling of the reservoirs to S , as well as the energy dependence of this coupling. We also assume locality (of Green's functions and density matrices). A physical justification for the latter approximation is the following. Assume that in each electrode there is a generic scattering mechanism with a scattering time τ . In the coherent-potential approximation electrons acquire a self-energy $-i\hbar/2\tau$ which shifts the poles of the Green's function off the real axis by that amount with the result that the Green's function becomes spatially localized on the scale of $l \sim v_F \tau$, where v_F is the Fermi velocity and l is the electron mean free path. The presence of such scatter-

ing in the electrodes would thus grant us the above locality.

Then

$$\begin{aligned} \frac{1}{i\hbar} [\hat{H}_S, \Delta\hat{\rho}_S] = & -\Gamma_1 \int_{\mu}^{\mu+eV/2} \hat{D}_S^{(1)}(E) dE \\ & + \Gamma_2 \int_{\mu-eV/2}^{\mu} \hat{D}_S^{(2)}(E) dE + \Gamma_1 \Delta\hat{\rho}_S^{(1)} + \Gamma_2 \Delta\hat{\rho}_S^{(2)}, \end{aligned}$$

where $\Gamma_j = 2 \text{Im}[\gamma_j] / \hbar$.

Our final approximation is

$$\begin{aligned} \int_{\mu}^{\mu+eV/2} \hat{D}_S^{(1)}(E) dE & \approx \hat{\rho}^{0(1)} - \bar{\rho}_S^{(1)}, \\ \int_{\mu-eV/2}^{\mu} \hat{D}_S^{(2)}(E) dE & \approx -(\hat{\rho}^{0(2)} - \bar{\rho}_S^{(2)}), \end{aligned}$$

where, as before, $\hat{\rho}^0$ is the initial, statically polarized, non-current-carrying density matrix in Eq. (2). Then

$$0 = \frac{1}{i\hbar} [\hat{H}_S, \Delta\hat{\rho}_S] - \Gamma_1 (\hat{\rho}_S^{(1)} - \hat{\rho}^{0(1)}) - \Gamma_2 (\hat{\rho}_S^{(2)} - \hat{\rho}^{0(2)}).$$

Now consider $[\hat{H}_S, \bar{\rho}_S]$. Using $\hat{D}_S(E) = \hat{G}_S^+(E) \hat{\sigma}_1(E) \hat{G}_S^-(E) / \pi + \hat{G}_S^+(E) \hat{\sigma}_2(E) \hat{G}_S^-(E) / \pi$,

$$\begin{aligned} [\hat{H}_S, \hat{D}_S] = & -\frac{1}{\pi} (\hat{\sigma}_1(E) \hat{G}_S^-(E) - \text{H.c.}) \\ & - \frac{1}{\pi} (\hat{\sigma}_2(E) \hat{G}_S^-(E) - \text{H.c.}) - (\hat{\Sigma}^+(E) \hat{D}_S(E) - \text{H.c.}), \end{aligned}$$

whence, with the approximation in Eq. (B3), $[\hat{H}_S, \hat{D}_S] = 0$. Hence, $[\hat{H}_S, \bar{\rho}_S] = 0$ and

$$0 = \frac{1}{i\hbar} [\hat{H}_S, \hat{\rho}_S] - \Gamma_1 (\hat{\rho}_S^{(1)} - \hat{\rho}^{0(1)}) - \Gamma_2 (\hat{\rho}_S^{(2)} - \hat{\rho}^{0(2)}).$$

This is a steady-state solution of Eq. (2) (with $\Gamma_1 = \Gamma_2 = \Gamma$), which is what we wished to show. As a broad indication, we see that the natural spatial regions of application of the damping in the finite open-boundary system are the exposed surfaces of the electrodes, and a typical strength for the parameter Γ is

$$\Gamma \sim 2\pi\beta^2 d / \hbar,$$

where β is a system-environment hopping integral and d is a surface LDOS per atom, in close agreement with the value used in the simulations above.

- ¹J. K. Tomfohr and O. F. Sankey, Phys. Status Solidi B **226**, 115 (2001).
- ²P. Orellana and F. Claro, Phys. Rev. Lett. **90**, 178302 (2003).
- ³A. P. Horsfield, D. R. Bowler, and A. J. Fisher, J. Phys.: Condens. Matter **16**, L65 (2004).
- ⁴G. Stefanucci and C.-O. Almbladh, Phys. Rev. B **69**, 195318 (2004).
- ⁵M. Di Ventra and T. N. Todorov, J. Phys.: Condens. Matter **16**, 8025 (2004).
- ⁶K. Burke, R. Car, and R. Gebauer, Phys. Rev. Lett. **94**, 146803 (2005).
- ⁷S. Kurth, G. Stefanucci, C.-O. Almbladh, A. Rubio, and E. K. U. Gross, Phys. Rev. B **72**, 035308 (2005).
- ⁸N. Bushong, N. Sai, and M. Di Ventra, Nano Lett. **5**, 2569 (2005).
- ⁹J. Pedersen and A. Wacker, Phys. Rev. B **72**, 195330 (2005).
- ¹⁰Y. Zhu, J. Maciejko, T. Ji, H. Guo, and J. Wang, Phys. Rev. B **71**, 075317 (2005).

- ¹¹R. Baer, T. Seideman, S. Ilani, and D. Neuhauser, *J. Chem. Phys.* **120**, 3387 (2004).
- ¹²M. A. Reed, J. Chen, A. M. Rawlett, D. W. Price, and J. M. Tour, *Appl. Phys. Lett.* **78**, 3735 (2001).
- ¹³A. P. Horsfield, D. R. Bowler, A. J. Fisher, T. N. Todorov, and C. G. Sánchez, *J. Phys.: Condens. Matter* **16**, 8251 (2004); *J. Phys.: Condens. Matter* **17**, 4793 (2005).
- ¹⁴D. R. Bowler, A. P. Horsfield, C. G. Sánchez, and T. N. Todorov, *J. Phys.: Condens. Matter* **17**, 3985 (2005).
- ¹⁵E. Runge and E. K. U. Gross, *Phys. Rev. Lett.* **52**, 997 (1984).
- ¹⁶A. Zangwill and P. Soven, *Phys. Rev. Lett.* **45**, 204 (1980); *Phys. Rev. B* **24**, 4121 (1981).
- ¹⁷This value of U corresponds to the difference between the ionization energy and electron affinity of the gold atom.
- ¹⁸J. B. Pendry, A. B. Prêtre, P. J. Rous, and L. Martin-Moreno, *Surf. Sci.* **244**, 160 (1991).
- ¹⁹T. N. Todorov, G. A. D. Briggs, and A. P. Sutton, *J. Phys.: Condens. Matter* **5**, 2389 (1993).
- ²⁰T. N. Todorov, J. Hoekstra, and A. P. Sutton, *Philos. Mag. B* **80**, 421 (2000).
- ²¹T. N. Todorov, *J. Phys.: Condens. Matter* **14**, 3049 (2002).
- ²²M. Brandbyge, J.-L. Mozos, P. Ordejón, J. Taylor, and K. Stokbro, *Phys. Rev. B* **65**, 165401 (2002).
- ²³M. Büttiker, Y. Imry, R. Landauer, and S. Pinhas, *Phys. Rev. B* **31**, 6207 (1985).
- ²⁴A 1D system can easily develop bound states outside the band. We have verified that for the self-consistent systems below there are no such states.
- ²⁵A. R. Rocha and S. Sanvito, *Phys. Rev. B* **70**, 094406 (2004).
- ²⁶N. Sai, M. Zwolak, G. Vignale, and M. Di Ventura, *Phys. Rev. Lett.* **94**, 186810 (2005).
- ²⁷K. Burke, M. Koentopp, and F. Evers, *Phys. Rev. B* **73**, 121403 (2006).